Supercooling of nanoscale Ga drops with controlled impurity levels

Eli A. Sutter, Peter W. Sutter, Emanuele Uccelli, and Anna Fontcuberta i Morral

Supercooling of nanoscale Ga drops with controlled impurity levels

Eli A. Sutter[1,*], Peter W. Sutter[1], Emanuele Uccelli[2,3], and Anna Fontcuberta i Morral[2,3]

[1]Center for Functional Nanomaterials, Brookhaven National Laboratory
Upton, New York 11973, USA

[2]Laboratoire des Matériaux Semiconducteurs, Institut des Matériaux, Ecole Polytechnique Fédérale de Lausanne, Switzerland

[3]Physik-Department and Walter Schottky Institut, Technische Universität München, 85748 Garching, Germany

*Corresponding author; e-mail: esutter@bnl.gov

Abstract

We use in-situ observations by variable temperature transmission electron microscopy on Ga drops at the tips of GaAs nanowires to investigate the phase behavior of nanoscale Ga. Experiments on pure Ga drops are compared with drops containing well-defined levels of impurities. Our controlled experiments for the first time show that the crystallization temperature, and hence the ultimate achievable supercooling, strongly depends on the concentration of impurities. All drops show predominant β- and γ-Ga correlations in the liquid phase and ultimately crystallize to solid β- and γ-Ga, which provides support for a scenario, in which impurities limit the achievable supercooling without significantly templating the crystalline phase.

Melting and crystallization are fundamental processes by which most substances change between a disordered liquid and an ordered solid state. When a liquid droplet is cooled, it reaches a point where it transforms into a solid. This point is not necessarily the equilibrium melting point. The possibility of significant supercooling in small droplets has been investigated extensively following the pioneering work of Turnbull [1]. It has been shown that small particles can melt and freeze at temperatures different from the bulk [2-4], undergo significantly higher supercooling [4], crystallize along different pathways [5], and in structures different from the bulk [6-11]. The extent of achievable supercooling can presumably vary with droplet size, purity [12], interactions with supports, etc. For most substances, the supercooling is limited to $\Delta T/T_M \sim 0.1 - 0.2$, where $\Delta T = T_M - T_C$ is the difference between the melting and crystallization temperatures [4]. Ga is a particular metal for which this value can be exceeded significantly, and thus Ga droplets have become a model system for studying deep supercooled liquids. Ga droplets can be supercooled to half of the melting temperature, $\Delta T/T_M \sim 0.5$, as demonstrated in different experiments on micro- and nanometer sized Ga in emulsions [13], and films of supported Ga droplets [8, 14]. Most of the investigations consider small encapsulated or confined Ga particles, and thus are affected by several factors at the same time: the effects of confined geometry and interactions with the confining matrix [7, 9, 15], uncontrolled levels of impurities, non-uniform droplet sizes, etc. An investigation of supercooled liquids and of their intrinsic crystallization pathway requires eliminating heterogeneous crystallization, e.g., due to contact with confining matrices and foreign materials. Limited ensemble measurements on films of supported Ga droplets indicate that very high supercooling may be achieved in small particles [14].

However, the Ga drops in these films were polydisperse and covered with SiO_2, and an ensemble measurement would not capture possible effects of particle size, shape, and support/matrix interactions on the highest achievable supercooling and crystallization pathway.

Here we investigate the crystallization and melting of Ga drops at the tips of GaAs nanowires (NWs). This particular geometry avoids any matrix effects, and limits the interactions between liquid Ga nanodroplets and the support surface to a well-defined solid-liquid interface. The use of *in-situ*, variable temperature transmission electron microscopy (TEM) allows us to follow the phase behavior of *individual* Ga droplets, among a large ensemble of similar NWs/drops confirming the generality of the observations on single drops. This unprecedented level of control allows us to perform identical experiments on pure Ga nanodroplets and on liquids containing different levels of impurities, to identify the effect of well-defined impurity concentrations on the achievable supercooling and crystallization of nanoscale Ga.

Our variable temperature *in-situ* experiments were carried out in a JEOL 2100F field emission TEM equipped with a Gatan liquid He cooling sample holder in the temperature range between 380 K and 10 K, at pressures below 2×10^{-7} Torr and low electron irradiation intensities (< 0.1 A/cm^2). Specimen temperatures were measured by a thermocouple, calibrated via the melting points of In and eutectic Au-Ge [10, 16, 17], and confirmed here via the melting temperature of Ga. Heating and cooling rates were slow (~5 K/min) to ensure efficient heat transfers and equilibration. The Ga/GaAs NW

structures were synthesized by molecular beam epitaxy as described in detail elsewhere [18]. Briefly, Ga-catalyzed growth was carried out at 630 °C on GaAs substrates covered with SiO_2. P-type doping of the NWs and different levels of Si in the Ga drops were achieved with the addition of a controlled silicon flux during the NW growth. In-situ TEM experiments were performed with Si-doped Ga droplets obtained using Si fluxes of 2.2×10^{10} and 1.6×10^{11} Si/cm^2 s, resulting in measured silicon concentrations in the NWs of 5.5×10^{18} and 4×10^{19} cm^{-3}, respectively [18, 19]. The Si concentration in the Ga droplets, $c_{Si(Ga)}$, is calculated from that of the NW, $c_{Si(NW)}$, via the distribution coefficient $k = c_{Si(NW)}/c_{Si(Ga)}$, which is well established for the Si-Ga(liquid)/GaAs(solid) system [18, 20]. Using values obtained in liquid phase epitaxy for our two doping levels gives Si concentrations in the liquid Ga droplets $c_{Si(Ga)}$ of 0.06 at. % and 0.47 at. %, to which we refer below as low- and high-doped Ga droplets. The NWs were transferred through air and dispersed on amorphous C films supported by Au grids. A thin amorphous oxide layer, initially visible on the Ga surface, desorbed during annealing of the samples to 450 K under the electron beam in the TEM [21].

Figure 1 a shows a characteristic TEM image of an undoped GaAs NW with a Ga drop at the tip. The striped contrast of the GaAs NW stems from its morphology, consisting of a sequence of segments with wurtzite and zincblende structure [22]. The Ga drops show darker contrast than the GaAs wires and appear as homogeneous spheres without any internal contrast at the NW tips. The NWs are initially heated to 350 K, then cooled slowly to 85 K while recording TEM images and electron diffraction patterns (DPs). The TEM image in figure 1 a, obtained at 94 K, is representative of the Ga drops over the

entire range from 350 K to 85 K. DPs (figure 1 b) over this temperature range consist of diffuse rings that indicate either a liquid or a glassy amorphous phase of the Ga drop. Further cooling of the drops to 12 K, using liquid He, results in crystallization of the Ga drop (figure 1 d, e) at a temperature between 85 K and 12 K. In the TEM image (figure 1 d) a change of contrast in the drop and facets on its surface are seen. The DP of the solidified Ga drop (figure 1 e) indicates that it is single crystalline and can be indexed to the metastable β-Ga phase with monoclinic structure [23]. For our pure Ga drops at the tips of the GaAs NWs, a crystallization temperature below 84 K implies a supercooling of at least $\Delta T/T_M \sim 0.7$ ($T_M^{\beta\text{-Ga}} = 256$ K, see below). Investigation of a large number of crystallized drops shows that the resulting solid Ga nanoparticles are mostly monocrystalline, and adopt either the metastable β- or γ-Ga phase. Some particles are polycrystalline. Ga drops on planar surfaces [8] and Ga encapsulated in carbon nanotubes [7] were found to crystallize in the same two metastable Ga phases that can even coexist in the same particle.

Following crystallization at T < 84 K, the temperature is increased and the Ga particles are heated slowly to room temperature. Melting generally occurs around 240 K. Upon melting the Ga drops recover their spherical shape with homogeneous contrast (figure 1 f). The DPs lose the discrete Bragg spots and again consist of diffuse rings, characteristic of the liquid state (figure 1 g). The DPs after melting are identical to the DPs of the initial drops before crystallization, and closely match the simulated DP for a liquid Ga drop with β-Ga like short-range correlations (figure 1 b). Real-space imaging never shows the characteristic contrast associated with an amorphous solid phase during heating or

cooling cycles, hence we conclude that the Ga particles change directly between liquid and crystalline solid phases.

To investigate the effect of controlled concentrations of impurities on the supercooling, crystallization, and melting, Ga drops with two different Si concentrations, 0.06 at. % and 0.47 at. %, are subjected to identical experiments. Even such small impurity concentrations influence significantly the crystallization temperatures of the Ga drops. Figure 2 shows variable temperature TEM images of highly doped Ga:Si drops with impurity levels of 0.47 at. %. The drops are originally liquid (figure 2 a, b), with DPs in the liquid state identical to those of our pure Ga drops. Upon decreasing the temperature crystallization occurs much sooner, i.e., at significantly higher temperatures than in the pure Ga drops. Ga drops with 0.47% Si content crystallize at (155 ± 5) K, whereas drops containing 0.06% Si crystallize at (144 ± 5) K (figure 3). In repeated experiments, the crystallization temperature, T_C, was determined by lowering T in 5 K steps, allowing the sample to equilibrate, and surveying an ensemble of Ga drops. Generally, all drops are still liquid at 5 K above the stated T_C, whereas all are crystalline at 5 K below, thus giving an error bar of $\pm$ 5 K. The melting temperatures, T_M, were determined analogously. A survey of a large number of drops shows the crystalline Ga particles again single crystalline or polycrystalline, in either the metastable β- or γ-Ga solid phases. The Ga drop shown in figure 2, for instance, crystallizes as γ-Ga (figure 2 e, f). Upon increasing the temperature all Ga particles (independent of Si content) melt in the interval between 230 K and 240 K. Figure 2 g, a TEM image at 230 K, shows the melted Ga drops, with a DP of diffuse rings (figure 2 h).

Our experiments on Ga drops with controlled impurity levels show that the concentration of Si impurities affects primarily the crystallization temperature of the Ga drops, but it does not lead to systematic changes in the melting temperature of the solid Ga particles (figure 3). Hence, the degree of supercooling, $\Delta T/T_M$, that can be achieved depends sensitively on the impurity level of the melt, varying from $\Delta T/T_M \sim 0.7$ for pure Ga drops to ~ 0.35 for drops with the highest Si content. The observation of melting temperatures only marginally below the melting temperatures of the bulk-like metastable β- and γ-Ga phases is consistent with the notion that melting, initiated as surface pre-melting, should not be affected strongly by size, support, and purity [16, 24].

The observed differences in supercooling between pure and doped Ga drops imply that the ultimate supercooling in the doped drops is limited by the presence of impurities. What, then, determines the achievable supercooling of the pure Ga melt? The NW-drop interface, for instance, could provide a template for heterogeneous nucleation of the crystalline phase in the drop. There are several factors that argue against this scenario. First, the facet at the NW tip, which can have either wurtzite or zincblende structure, does not induce a particular orientation of the crystallized Ga particles. Analyzing the DPs of many particles after crystallization, we detect no particular alignment of the Ga lattice relative to the NW. As noted, in some cases the particles are even polycrystalline after freezing, suggesting several crystallization centers. Second, to further investigate possible support effects, some of the Ga drops were severed from the tips of the GaAs NWs and distributed on the amorphous C films of the TEM grid (figure 4). Such amorphous C

supported drops show crystallization and melting identical to the drops held at the NW tips. In particular, the freezing and melting temperatures, and hence the extent of supercooling, are the same as for NW-supported drops, suggesting that the observed differences in supercooling are robust and independent of the support. Thus, the supercooling of our pure Ga drops is determined either by heterogeneous nucleation involving a very low level of residual impurities, by homogeneous nucleation [25], or by surface-induced crystallization [5].

Both pure and Si-doped Ga drops – at the NW tips as well as on amorphous C – invariably crystallize in either the β- or the γ-Ga metastable phases, but not in the stable bulk phase, α-Ga. As the crystal structure and orientation is not determined by the support interface, it is possible that short-range correlations in the Ga liquid provide a template for the crystalline phase, especially for the pure Ga drops that show extreme supercooling. A diffraction analysis on individual liquid drops is used to investigate this possibility. Figure 5 a shows the radial distributions of the diffracted intensity of pure and doped Ga drops at two different temperatures. The principal feature is a peak with a shoulder towards larger wave vectors, consistent with x-ray diffraction patterns of liquid Ga [26, 27]. The diffraction features do not change significantly with temperature or purity, except for a slight thermal (Debye-Waller) broadening at higher temperatures. Figure 5 b shows calculated structure factors of the α-, β- and γ-Ga phases [23, 28, 29], computed with an ab-initio powder pattern simulation as implemented in the software package JEMS [30]. Both β- and γ-Ga have structure factors nearly identical to the experimentally observed diffraction intensities, in particular the characteristic primary

peak at ~4 nm^{-1} and a shoulder toward higher spatial frequencies. α-Ga is clearly different, and shows a minimum at 4 nm^{-1} with peaks on either side. If α-Ga correlations exist in our Ga drops, figure 5 shows that they clearly constitute a minority structure, with the majority being β- and γ-Ga-like. The short-range structural motifs observed in the liquid Ga drops in our experiments could act as precursors of the crystalline β- and γ-Ga phases. The fact that all of our drops – irrespective of impurities – show β- and γ-Ga correlations in the liquid phase and ultimately crystallize to solid β- and γ-Ga provides strong support for a scenario, in which the crystalline phase is templated by short-range order in the liquid phase, and not by external factors such as a particular support structure (both GaAs and amorphous C supports give the same results) [31] or a nucleation center involving impurities in the bulk [32] or on the surface [33]. We can thus conclude that impurities in the melt (e.g., Si in liquid Ga) can constitute crystallization centers that limit the achievable supercooling, while the structure of the incipient solid is determined by the particular structural motifs of the liquid metal itself. Our results show strong similarities with previous work on Ti-Zr-Ni alloys, which concluded that icosahedral short-range order in the supercooled liquid is responsible for the nucleation of a *metastable* crystalline icosahedral (quasicrystal) phase instead of the stable solid phase [11]. While this previous work supported Frank's hypothesis [25] that icosahedral short-range order stabilizes the liquid phase and promotes deep supercooling, our results on deep supercooled elemental Ga suggest that other structural motifs in the liquid – similar to the structure of the *metastable* β- and γ-Ga – may play an analogous role. This raises the possibility that short-range motifs other than the accepted icosahedral one (and perhaps especially those close to a metastable structure of the solid) can stabilize deep
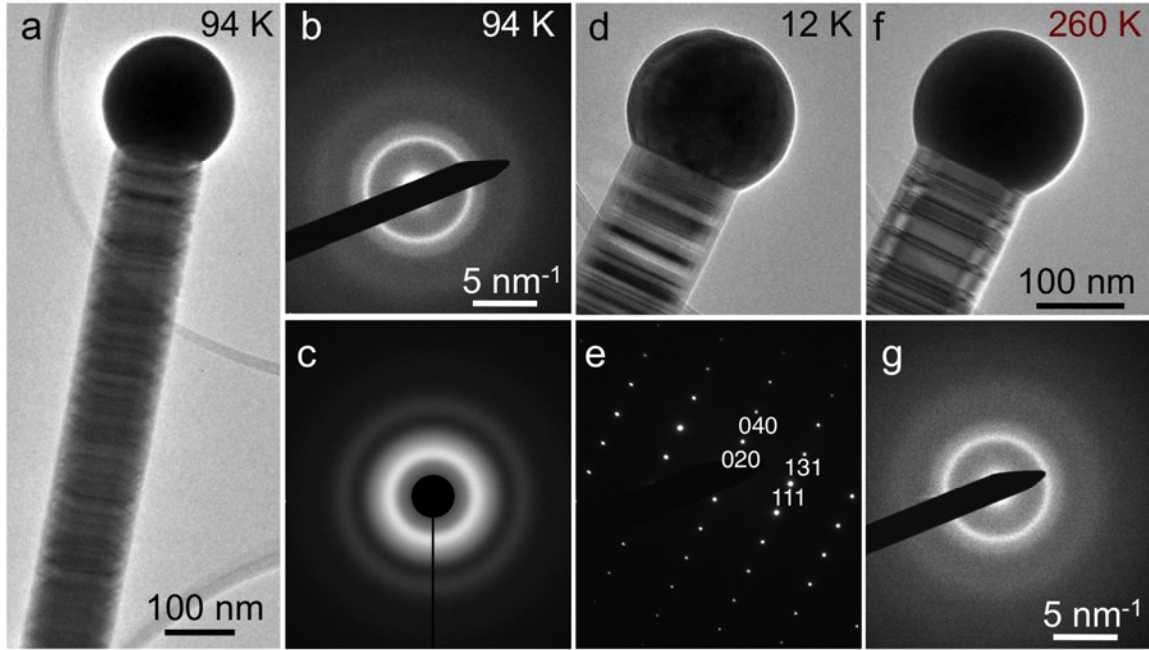
supercooled liquids.

Acknowledgements

Figure 1: Crystallization and melting of pure Ga drops at the tips of GaAs nanowires. Crystallization of a Ga drop: a – TEM image of the GaAs nanowire with Ga drop at its tip during cooling from room temperature (T = 94 K). **b** – Diffraction pattern from the Ga drop at 94 K exhibiting diffuse rings. **c** – Simulated diffraction pattern for a liquid with β-Ga short-range structure. **d, e** – TEM image of the single-crystalline β-Ga particle at 12 K and the corresponding diffraction pattern along the [-101] zone axis. **Melting of the Ga particle: f, g** –TEM image and diffraction pattern of the Ga drop after melting (T = 260 K) during heating from 12 K.
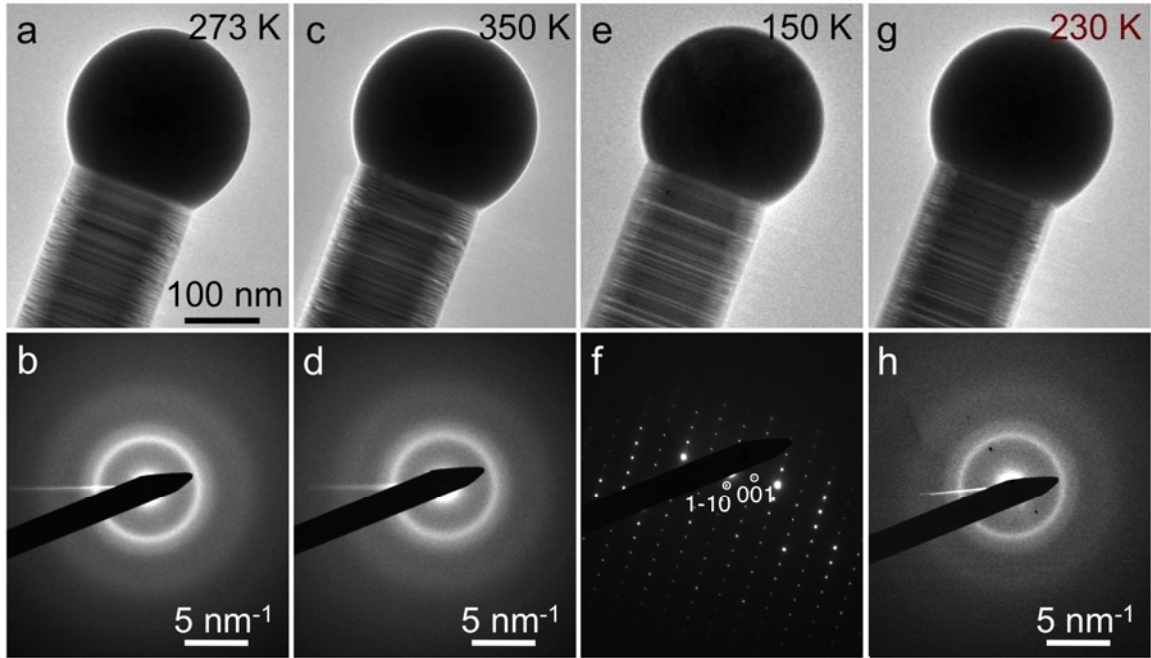
Figure 2: Crystallization and melting of highly Si-doped Ga drops at the tips of GaAs nanowires. Crystallization of the Ga drop: a – TEM image of the GaAs nanowire and Ga drop at its tip at room temperature. **b –** Diffraction pattern from the Ga drop at room temperature exhibiting diffuse rings, characteristic of a liquid. **c, d –** TEM image of the and diffraction pattern from the Ga drop during a brief heating to 350 K, prior to cooling. **e, f –** TEM image of the single crystalline γ-Ga particle at 150 K and the corresponding diffraction pattern along the [110] zone axis. **Melting of the Ga particle: g, h –**TEM image and diffraction pattern of the Ga drop after melting (T = 230 K) during heating from 90 K.
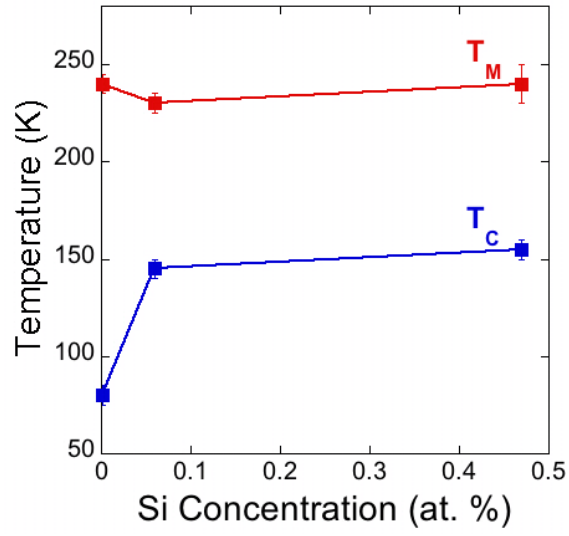
Figure 3: Dependence of the melting (T_M) and crystallization (T_C) temperature of Ga

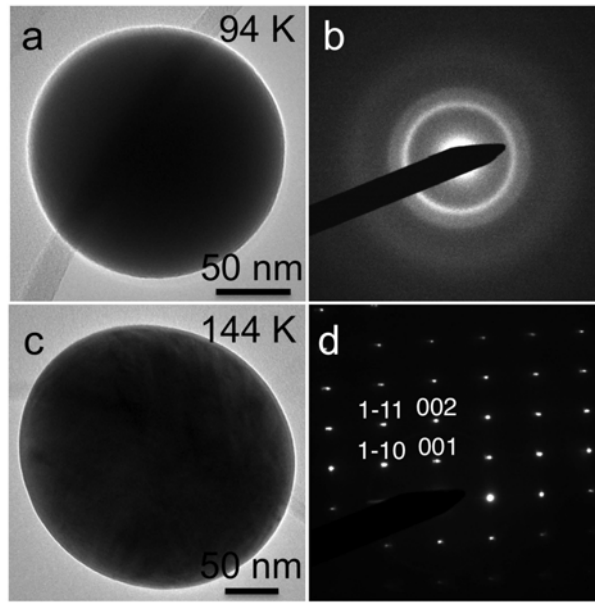drops at the tips of GaAs NWs on the Si impurity concentration.

Figure 4: Crystallization of pure and Si-doped Ga drops on amorphous carbon films. a – TEM image of a pure Ga drop during cooling from room temperature (image recorded at T = 94 K). **b –** Diffraction pattern of the pure Ga drop at 94 K exhibiting diffuse rings, characteristic of a liquid. **c, d –** TEM image and corresponding diffraction pattern of a Si-doped Ga drop that has crystallized at 144 K. The diffraction pattern of the single crystalline Ga particle can be indexed to β-Ga with [110] zone axis.
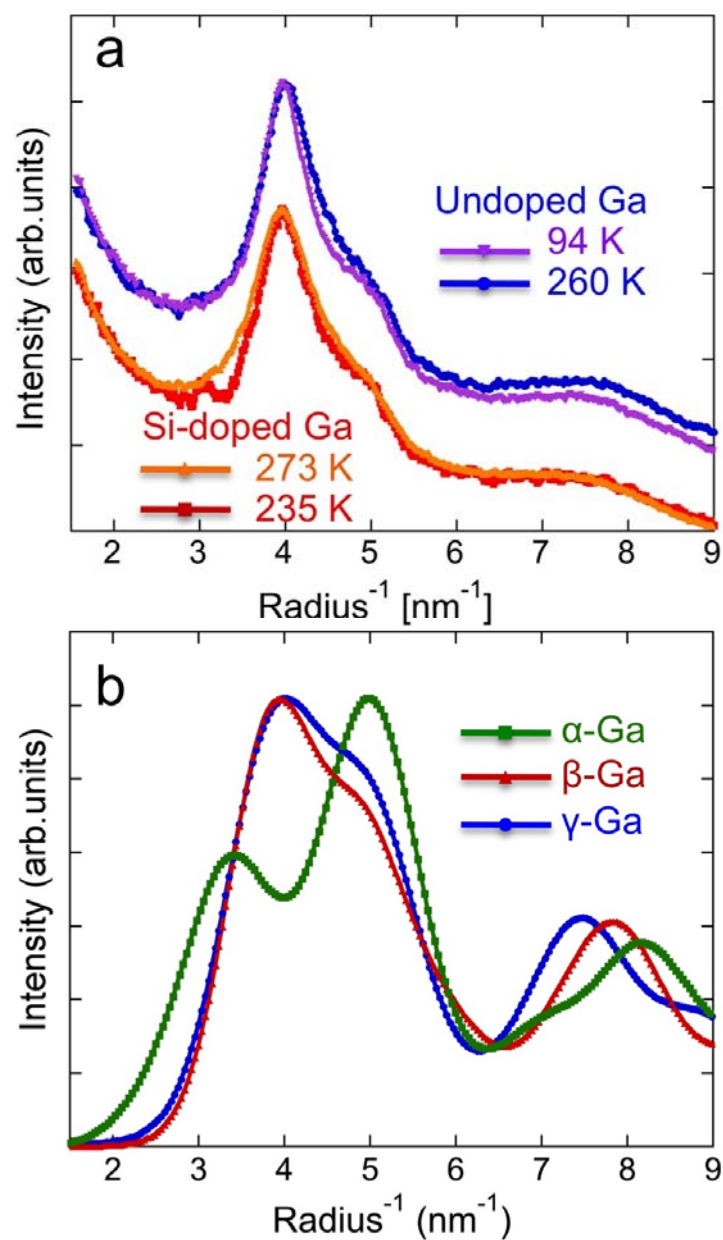
Figure 5: Electron diffraction of the liquid Ga drops. a – Radial distribution of the diffracted intensity of the pure and Si-doped liquid Ga drops at different temperatures. **b** – Calculated structure factors of the α-, β- and γ-Ga phases

References:

[1] D. Turnbull, The Subcooling of Liquid Metals, J Appl Phys, 20 (1949) 817-817.

[2] A.N. Goldstein, C.M. Echer, A.P. Alivisatos, Melting in Semiconductor Nanocrystals, Science, 256 (1992) 1425-1427.

[3] C.Q. Sun, Size dependence of nanostructures: Impact of bond order deficiency, Prog Solid State Ch, 35 (2007) 1-159.

[4] D. Turnbull, R.E. Cech, Microscopic Observation of the Solidification of Small Metal Droplets, J Appl Phys, 21 (1950) 804-810.

[5] P.W. Sutter, E.A. Sutter, Dispensing and surface-induced crystallization of zeptolitre liquid metal-alloy drops, Nat Mater, 6 (2007) 363-366.

[6] A.d. Cicco, Phase Transitions in Confined Gallium Droplets, Phys Rev Lett, 81 (1998) 2942-2945.

[7] Z.W. Liu, Y. Bando, M. Mitome, J.H. Zhan, Unusual freezing and melting of gallium encapsulated in carbon nanotubes, Phys Rev Lett, 93 (2004) 095504.

[8] S. Pochon, K.F. MacDonald, R.J. Knize, N.I. Zheludev, Phase coexistence in gallium nanoparticles controlled by electron excitation, Phys Rev Lett, 92 (2004) 145702-145705.

[9] E.V. Charnaya, C. Tien, K.J. Lin, Y.A. Kumzerov, X-ray studies of the melting and freezing phase transitions for gallium in a porous glass, Phys Rev B, 58 (1998) 11089-11092.

[10] E. Sutter, P. Sutter, Formation and stabilization of single-crystalline metastable AuGe phases in Ge nanowires Nanotechnology, 22 (2011) 295605.

[11] K.F. Kelton, G.W. Lee, A.K. Gangopadhyay, R.W. Hyers, T.J. Rathz, J.R. Rogers, M.B. Robinson, D.S. Robinson, First x-ray scattering studies on electrostatically levitated metallic liquids: Demonstrated influence of local icosahedral order on the nucleation barrier, Phys Rev Lett, 90 (2003).

[12] W.H. Hofmeister, C.W. Morton, R.J. Bayuzick, A.J. Rulison, J.L. Watkins, The kinetics of solid nucleation in zirconium, Acta Mater, 46 (1998) 6033-6039.

[13] L. Bosio, C.G. Windsor, Observation of a Metastability Limit in Liquid Gallium, Phys Rev Lett, 35 (1975) 1652-1655.

[14] G.B. Parravicini, A. Stella, P. Ghigna, G. Spinolo, A. Migliori, F. d'Acapito, R. Kofman, Extreme undercooling (down to 90 K) of liquid metal nanoparticles, Appl Phys Lett, 89 (2006) 033123-033125.

[15] M.K. Lee, C. Tien, E.V. Charnaya, H.S. Sheu, Y.A. Kumzerov, Structural variations in nanosized confined gallium, Phys Lett A, 374 (2010) 1570-1573.

[16] E. Sutter, P. Sutter, Phase diagram of nanoscale alloy particles used for vapor-liquid-solid growth of semiconductor nanowires, Nano Lett, 8 (2008) 411-414.

[17] E.A. Sutter, P.W. Sutter, Size-Dependent Phase Diagram of Nanoscale Alloy Drops Used in Vapor-Liquid-Solid Growth of Semiconductor Nanowires, Acs Nano, 4 (2010) 4943-4947.

[18] J. Dufouleur, C. Colombo, T. Garma, B. Ketterer, E. Uccelli, M. Nicotra, A.F.I. Morral, P-Doping Mechanisms in Catalyst-Free Gallium Arsenide Nanowires, Nano Lett, 10 (2010) 1734-1740.

[19] B. Ketterer, E. Mikheev, E. Uccelli, A.F.I. Morral, Compensation mechanism in silicon-doped gallium arsenide nanowires, Appl Phys Lett, 97 (2010) 223103.

[20] S.J. Moss, A. Ledwith, Chemistry of the Semiconductor Industry, Chapman and Hall, New York, 1997.

[21] E. Sutter, P. Sutter, Au-Induced Encapsulation of Ge Nanowires in Protective Carbon Shells, Adv Mater, 18 (2006) 2583.

[22] D. Spirkoska, J. Arbiol, A. Gustafsson, S. Conesa-Boj, F. Glas, I. Zardo, M. Heigoldt, M.H. Gass, A.L. Bleloch, S. Estrade, M. Kaniber, J. Rossler, F. Peiro, J.R. Morante, G. Abstreiter, L. Samuelson, A.F.I. Morral, Structural and optical properties of high quality zinc-blende/wurtzite GaAs nanowire heterostructures, Phys Rev B, 80 (2009) 245325.

[23] L. Bosio, A. Defrain, H. Curien, A. Rimsky, Crystal Structure of Beta-Gallium, Acta Crystall B-Stru, B 25 (1969) 995-996.

[24] J.W.M. Frenken, J.F. Vanderveen, Observation of Surface Melting, Phys Rev Lett, 54 (1985) 134-137.

[25] F.C. Frank, Supercooling of Liquids, Proc R Soc Lon Ser-A, 215 (1952) 43-46.

[26] A. Bizid, L. Bosio, H. Curien, A. Defrain, M. Dupont, X-Ray-Diffraction Study of Liquid Gallium between +50 and -110 Degrees C, Phys Status Solidi A, 23 (1974) 135-145.

[27] A. Bizid, L. Bosio, R. Cortes, X-Ray-Diffraction Study of Liquid Gallium Structure at 323 and 203k, J Chim Phys Pcb, 74 (1977) 863-865.

[28] Blanconn.P, L. Bosio, A. Defrain, A. Rimsky, H. Curien, Etude Cristallographique Dune Nouvelle Forme Metastable Du Gallium - Le Gallium Gamma, B Soc Fr Mineral Cr, 88 (1965) 145-146.

[29] B.D. Sharma, J. Donohue, A refinement of the crystal structure of gallium, Zeitschrift fuer kristallographie, kristallgeometrie, kristalchemie, 117 (1962) 293-300.

[30] http://cimewww.epfl.ch/people/stadelmann/jemsWebSite/jems.html.

[31] A.L. Greer, Liquid metals: Supercool order, Nat Mater, 5 (2006) 13-14.

[32] M. Volmer, Kinetik der Phasenbildung. , Steinkopff, Leipzig, 1939.

[33] V. Halka, R. Streitel, W. Freyland, Is surface crystallization in liquid eutectic AuSi surface-induced?, J Phys-Condens Mat, 20 (2008) 355007.